Post-print version of paper by Castaneda-Zegarra et al., published in DNA repair journal (Amst.) 2019 Jan;73:164-169. doi: 10.1016/j.dnarep.2018.12.002. Epub 2018 Dec 16. PMID: 30579708

Synthetic lethality between DNA repair factors *Xlf* and *Paxx* is rescued by inactivation of *Trp53*

Sergio Castañeda-Zegarra[1,2,3], Mengtan Xing[1,2], Raquel Gago-Fuentes[1,2], Siri Sæterstad[1,2], and Valentyn Oksenych*[1,2]

[1]Department of Clinical and Molecular Medicine, Norwegian University of Science and Technology, Laboratory Center, Erling Skjalgssons gate 1, 7491 Trondheim, Norway

[2]St. Olavs Hospital, Trondheim University Hospital, Clinic of Medicine, Postboks 3250 Sluppen, 7006 Trondheim

[3]Department of Biomedicine, University of Bergen, Bergen, Norway

Key words: synthetic lethality; genetic interaction; SCID; B lymphocyte; Cernunnos

*Corresponding authors:

valentyn.oksenych@ntnu.no (Valentyn Oksenych)

Post-print version of paper by Castaneda-Zegarra et al., published in DNA repair journal (Amst.) 2019 Jan;73:164-169. doi: 10.1016/j.dnarep.2018.12.002. Epub 2018 Dec 16. PMID: 30579708

Abstract

Non-homologous end joining (NHEJ) is a DNA repair pathway that senses, processes and ligates DNA double-strand breaks (DSBs) throughout the cell cycle. During NHEJ, core Ku70 and Ku80 subunits bind DSBs as a heterodimer and promote further recruitment of accessory factors (e.g., PAXX, Mri, DNA-PKcs, Artemis) and downstream core subunits XRCC4 and DNA ligase 4 (Lig4). Inactivation of *Ku70* or *Ku80* genes in mice results in immunodeficiency and high levels of genomic instability; deletion of individual *Dna-pkcs*, *Xlf*, *Paxx* or *Mri* genes results in viable mice with no or modest DNA repair defects. However, combined inactivation of either *Xlf* and *Dna-pkcs*, or *Xlf* and *Paxx,* or *Xlf* and *Mri*, leads to synthetic lethality in mice, which correlates with increased levels of apoptosis in the central nervous system. Here, we demonstrated that inactivation of pro-apoptotic factor *Trp53* rescues embryonic lethality of *Xlf*$^{-/-}$*Paxx*$^{-/-}$ and *Xlf*$^{-/-}$*Dna-pkcs*$^{-/-}$ double knockout mice. Moreover, combined inactivation of *Paxx* and *Dna-pkcs* results in live-born fertile *Paxx*$^{-/-}$*Dna-pkcs*$^{-/-}$ mice indistinguishable from *Dna-pkcs*$^{-/-}$ knockout controls.

1. Introduction

DNA double-strand breaks (DSBs) are recognized, processed and ligated by non-homologous DNA end joining (NHEJ) throughout the cell cycle [1]. Ku70/Ku80 heterodimer is the core NHEJ component that senses DSBs and facilitates recruitment of downstream NHEJ factors. Other NHEJ core factors, DNA ligase 4 (Lig4) and X-ray repair cross-complementing protein 4 (XRCC4) are involved in DNA end ligation. There are several accessory NHEJ proteins, including DNA-dependent protein kinase, catalytic subunit (DNA-PKcs), Artemis, XRCC4-like factor (XLF, or Cernunnos), paralogue of XRCC4 and XLF (PAXX, or XLS) and the modulator of retroviral infection (MRI, or Cyren) [1-5].

In order to investigate the role of NHEJ factors *in vivo*, multiple transgenic mouse models were developed and characterized. Inactivation of both alleles of Ku70 [6] or Ku80 [7] results in live-born mice that possess immunodeficiency and high levels of genomic instability [6-11]. Contrary, inactivation of *Xrcc4* [12] or *Lig4* [13] results in embryonic lethality that correlates with apoptosis in the central nervous system (CNS). Inactivation of an accessory NHEJ factor results in modest or no detectable phenotype in mice. In particular, knockout of *Dna-pkcs* [14] results in severe combined immunodeficiency (SCID) and increased levels of genomic instability [10, 11], while inactivation of *Xlf* leads to modest reduction of lymphocyte count and increased proportion of spontaneous chromosomal breaks [9-11, 15, 16]. Mice lacking either *Paxx* [8, 17-20] or *Mri* ([3]; and our unpublished observations) do not possess any detectable phenotype.

More recently, a number of studies demonstrated that XLF is functionally redundant with accessory NHEJ factors such as DNA-PKcs [10], PAXX [17-19] and Mri [3], which challenged study of DNA-PKcs, XLF, PAXX and Mri functions *in vivo*. Previously, we demonstrated that inactivation of either both alleles of *Ku70* or one allele of *Trp53* rescued synthetic lethality between *Xlf* and *Dna-pkcs* [11]. However, it was unclear whether synthetic lethality between *Xlf* and *Paxx* is Trp53-dependent.

Here, we demonstrated that genetic inactivation of one or two *Trp53* alleles has rescued synthetic lethality between *Xlf* and *Paxx* leading to immunodeficient phenotype; moreover, combined inactivation of *Paxx* and *Dna-pkcs* resulted in viable mice indistinguishable from *Dna-pkcs* knockout controls.

2. Material and Methods

2.1. Mouse models

All experiments involving mice were performed according to the protocols approved by Norwegian University of Science and Technology (NTNU). *Xlf*$^{+/-}$ [15], *Paxx*$^{+/-}$ [8], *Trp53*$^{+/-}$ [21], *Ku80*$^{+/-}$ [7], *Dna-pkcs*$^{+/-}$ [14], *Dna-pkcs*$^{scid/scid}$ [22] and *Mdc1*$^{+/-}$ [23] mice were previously described.

2.2. Lymphocyte count

For *ex vivo* lymphocyte examination, the mice were euthanized, and spleens and thymi were extracted. The organs were homogenized and cells were treated with red blood cell lysing buffer Hybri-Max™ (Sigma Aldrich, UK) for 5 minutes on ice. The total amount of splenocytes and thymocytes was determined using Trypan Blue Stain (0.4%) (Life Technologies, USA) and Countess II FL Automated Cell Counter (Life Technologies, USA).

2.3. DSB sensitivity assay

Human haploid HAP1 cells were custom-generated by *Horizon Discovery Group* (Waterbeach, UK) and are commercially available. According to the manufacturer's instructions, HAP1 cells were cultured in Iscove's Modified Dulbecco's Medium (IMDM, ThermoFisher, 21980065) supplemented with 10% Fetal Bovine Serum (FBS, Sigma, F7524) and 1% Penicillin-Streptomycin (ThermoFisher, 15140122) at 37°C with 5% CO_2. During the assays, Doxorubicin (Selleckchem, S1208), Bleomycin (Selleckchem, S1214), and PrestoBlue™ Cell Viability Reagent (ThermoFisher, A13262) were used.

HAP1 cells' sensitivity to DSB-inducing reagents (doxorubicin or bleomycin) was measured with PrestoBlue, according to the manufacturer's instructions. Briefly, on day 0, 2000 cells per well were seeded into 96-well plates, in 100µL IMDM media; on day 1, 50µL of media was removed and 50µL of fresh media containing indicated doses of doxorubicin or bleomycin was added to the wells. Each concentration point was performed in triplicates. On day 4, 11µL of PrestoBlue reagent (10×) was added to the wells; after 30 minutes incubation at 37°C, the cellular viability was measured with a fluorescence multi-well reader, using the excitation/emission wavelengths set at 544/590nm.

3. Results

3.1. Inactivation of *Trp53* gene rescues embryonic lethality of *Xlf*$^{-/-}$*Paxx*$^{-/-}$ mice

By intercrossing mice homozygous for *Xlf* null allele and heterozygous for *Paxx* (*Xlf*$^{-/-}$*Paxx*$^{+/-}$) we did not detect any live-born double knockout *Xlf*$^{-/-}$*Paxx*$^{-/-}$ mice (Figure 1A). However, alive double knockout *Xlf*$^{-/-}$*Paxx*$^{-/-}$ embryos were detected at embryonic day E15.5 (Figure 1B), in line with previously published observations [17-19]. To determine if this embryonic lethality is Trp53-dependent, we next intercrossed mice homozygous for *Xlf* null allele and heterozygous for both *Paxx* and *Trp53* (*Xlf*$^{-/-}$*Paxx*$^{+/-}$ *Trp53*$^{+/-}$). Strikingly, triple null *Xlf*$^{-/-}$*Paxx*$^{-/-}$*Trp53*$^{-/-}$ mice were live-born (Figure 1C). *Xlf*$^{-/-}$*Paxx*$^{-/-}$*Trp53*$^{-/-}$ triple knockout mice were significantly smaller than age-matched wild-type (WT) and single knockout controls ($p<0.0001$), and resembled *Ku80*$^{-/-}$ mice of similar age (Figure 1D, E). Triple knockout *Xlf*$^{-/-}$*Paxx*$^{-/-}$*Trp53*$^{-/-}$ mice had reduced size of spleens and thymi (Figure 1F,G,H) and only background levels of splenocytes and thymocytes, with cell levels similar to SCID phenotypes, e.g. *Ku80*$^{-/-}$ (Figure 1I, J). In addition, *Xlf*$^{-/-}$*Paxx*$^{-/-}$*Trp53*$^{-/-}$ mice were viable up to 60 days and died for unknown reasons. No tumors were detected in these triple knockout mice during the indicated period of time. *Xlf*$^{-/-}$*Paxx*$^{-/-}$*Trp53*$^{+/-}$ mice were also live-born, possessed reduced body weight, reduced size of spleens and thymi and severe lymphocytopenia (Figure 1). We concluded that synthetic lethality between *Xlf* and *Paxx* is Trp53-dependent.

3.2. Inactivation of *Trp53* rescues embryonic lethality of *Xlf*$^{-/-}$*Dna-pkcs*$^{-/-}$ mice

Upon inbreeding mice homozygous for *Xlf* null allele and heterozygous for both *Dna-pkcs* and *Trp53* (*Xlf*$^{-/-}$*Dna-pkcs*$^{+/-}$*Trp53*$^{+/-}$), we found that haploinsufficiency for *Trp53* rescues synthetic lethality between *Xlf* and *Dna-pkcs* genes. *Xlf*$^{-/-}$*Dna-pkcs*$^{-/-}$*Trp53*$^{+/-}$ mice possessed reduced body weight and lifespan when compared to gender and age-matched WT and single knockout controls (Figure 2)[11]. These *Xlf*$^{-/-}$*Dna-pkcs*$^{-/-}$*Trp53*$^{+/-}$ mice survived between 60 and 240 days and did not show any signs of tumors including lymphoma. Similar to *Dna-pkcs*$^{-/-}$ single knockouts, these mice possessed SCID phenotype (Figure 2). Surprisingly, by analyzing 328 live-born mice at postnatal day 30, only one *Xlf*$^{-/-}$*Dna-pkcs*$^{-/-}$*Trp53*$^{-/-}$ triple knockout mouse was detected, which is about twenty times less frequent than one could expect based on Mendelian distribution (1:2:1:2:4:2:1:2:1) (Figure 2A). This *Xlf*$^{-/-}$*Dna-pkcs*$^{-/-}$*Trp53*$^{-/-}$ mouse died at postnatal day 55. *Post mortem* analyzes revealed signs of lymphoma, including three large lymph nodes (303mg total weight), and large spleen (160mg). In addition, we analyzed 112 pups at postnatal day 1, and no live-born triple knockout mice were detected in this group (Figure 2B). We concluded that synthetic lethality between *Xlf* and *Dna-pkcs* is Trp53-dependent. Further analyzes are required to determine the reasons of lack of live-born *Xlf*$^{-/-}$*Dna-pkcs*$^{-/-}$*Trp53*$^{-/-}$ triple knockout mice.

3.3. Double knockout mice deficient for *Paxx* and *Dna-pkcs* are live-born

Simultaneous inactivation of either *Xlf* and *Dna-pkcs* (*Xlf*$^{-/-}$*Dna-PKcs*$^{-/-}$), or *Xlf* and *Paxx* (*Xlf*$^{-/-}$*Paxx*$^{-/-}$) genes resulted in synthetic lethality in mice [10, 11, 17-19], suggesting that XLF has overlapping or complementary functions with both DNA-PKcs and PAXX. However, it was unclear whether DNA-PKcs and PAXX complement each other during the mouse development. Here, we intercrossed mice homozygous for *Paxx* null allele [8] and heterozygous for *Dna-pkcs* [14] (*Paxx*$^{-/-}$*Dna-pkcs*$^{+/-}$). We obtained viable double knockout *Paxx*$^{-/-}$*Dna-pkcs*$^{-/-}$ mice at expected proportions (28 : 63 : 26, which is close to 1 : 2 : 1). Double knockout *Paxx*$^{-/-}$*Dna-pkcs*$^{-/-}$ mice were indistinguishable from the *Dna-pkcs*$^{-/-}$ age-matched controls (Figure 3). Moreover, mice lacking both PAXX and DNA-PKcs were fertile and had no detectable defects except immunodeficiency. In addition, we intercrossed mice homozygous for *Paxx* null allele and heterozygous for a mutation in *Dna-pkcs* gene resulting in SCID phenotype due to C-terminal alteration [22], *Paxx*$^{-/-}$*DNA-PKcs*$^{+/scid}$. Double deficient *Paxx*$^{-/-}$*Dna-pkcs*$^{scid/scid}$ mice were also viable and indistinguishable from *Dna-pkcs*$^{scid/scid}$ age-matched controls (Figure 3 and data not shown). We concluded that there is no obvious functional redundancy between DNA repair factors PAXX and DNA-PKcs in mouse development.

To establish whether the combination of PAXX and DNA-PKcs deficiencies leads to an increased general NHEJ defect, we performed cell sensitivity assays to DSBs-inducing factors doxorubicin and bleomycin (Figure 3). Inactivation of *PAXX* alone did not change cellular sensitivity to both DSB-inducing reagents when compared to WT controls (n.s., p>0,2414). Inactivation of *DNA-PKcs* and combined inactivation of *DNA-PKcs* and *PAXX* resulted in hypersensitivity to doxorubicin and bleomycin. However, there was no significant difference between the viability of DNA-PKcs-deficient and DNA-PKcs/PAXX double-deficient cells to the DSBs (n.s., p>0,8173). Inactivation of core NHEJ factor XRCC4 (Figure 3) or Lig4 (not shown) resulted in the highest DSB-sensitivity in cells, although not significantly different from the DNA-PKcs-deficient or PAXX/DNA-PKcs double-deficient lines (n.s., p>0,1392). These observations highlight a previous report stating no detectable genetic interaction between *DNA-PKcs* and *PAXX* in mammalian cells [24].

4. Discussion

Knockout or haploinsufficiency for *Trp53* rescued embryonic lethality of *Xrcc4*$^{-/-}$ [12, 25] and *Lig4*$^{-/-}$ [13, 26] mice likely due to reduced apoptosis in the central nervous system. While knockout of *Xlf*, *Dna-pkcs*, *Paxx* or *Mri* resulted in no obvious defect in neurodevelopment, combined inactivation of *Xlf* and

Paxx (*Xlf*$^{-/-}$*Paxx*$^{-/-}$) [17-19], or *Xlf* and *Mri* (*Xlf*$^{-/-}$*Mri*$^{-/-}$) [3], resulted in severe neuronal apoptosis in murine brain during embryonic development. It suggests that XLF indeed has a role in neurodevelopment, and this role is compensated by other factors, e.g. accessory NHEJ proteins DNA-PKcs, PAXX, and Mri. In addition, mice homozygous for *Dna-pkcs* gene carrying point mutation (D3922A) resulted in lethal phenotype with increased neuronal apoptosis [27], confirming that DNA-PKcs is also involved in neurodevelopment. Inactivation of one or two alleles of *Trp53* might result in reduced cellular apoptosis in *Xlf*$^{-/-}$*Paxx*$^{-/-}$ mice allowing postnatal survival (Figure 1). Similarly, *Xlf*$^{-/-}$*Dna-pkcs*$^{-/-}$*Trp53*$^{+/-}$ mice likely survived due to reduced apoptosis. However, it is not clear why *Xlf*$^{-/-}$*Dna-pkcs*$^{-/-}$*Trp53*$^{-/-}$ mice were not detected among the live-born pups at the expected ratio. A similar observation was made with mice deficient for a DNA-PKcs-related protein kinase, ataxia telangiectasia mutated and rad3 related (ATR). Inactivation of *Trp53* did not rescue the severe phenotype of Seckel syndrome mouse model with mutated *Atr* gene [28]. In particular, *Atr*$^{Seckel/Seckel}$*Trp53*$^{-/-}$ double mutant mice were born 6 times less often than expected, 1% instead of 6%. In addition, inactivation of *Trp53* did not rescue embryonic lethality of mice deficient for *antipolo-like kinase 1 (PLK1)-interacting checkpoint helicase* (*Pich*$^{-/-}$), suggesting that genomic instability-associated embryonic lethality is not always p53-dependent [29]. Overall, it is possible that the early lethality of live-born *Xlf*$^{-/-}$*Dna-Pkcs*$^{-/-}$*Trp53*$^{+/-}$, *Xlf*$^{-/-}$*Paxx*$^{-/-}$*Trp53*$^{+/-}$ and *Xlf*$^{-/-}$*Paxx*$^{-/-}$*Trp53*$^{-/-}$ mice correlates with accelerated aging, and this option requires additional study.

Combined inactivation of *Xlf* and *Paxx* in progenitor B cell lines resulted in V(D)J recombination block *ex vivo* [30-32]. It was however unclear whether combined inactivation of *Xlf* and *Paxx* will result in lack of B and T lymphocytes in adult mice due to synthetic lethality between the *Xlf* and *Paxx* genes [17-19]. Here, we demonstrated that mice lacking XLF and PAXX, although live-born in the absence of one or two alleles of *Trp53* possess no B and T lymphocytes. Similar triple knockout mouse model might be used in an attempt to overcome synthetic lethality between other genes, for example, *Xlf* and *Mri* (Hung et al., 2018).

Previously, an *Xlf*$^{-/-}$ mouse model was used to demonstrate that ATM kinase and ATM-dependent DNA damage response factors are required for efficient lymphocyte development, and mouse development in general. Combined inactivation of *Xlf* and *Atm*, or *Xlf* and *53bp1*, resulted in live-born mice with nearly no mature B and T lymphocytes, high levels of genomic instability and reduced body weight [1, 9, 33, 34]. More strikingly, combined inactivation of *Xlf* and *histone H2ax*, or *Xlf* and *Mediator of DNA damage checkpoint 1 (Mdc1)*, resulted in early synthetic lethality in mice ([34] and own observations). Specifically, by inter-breeding *Xlf*$^{-/-}$*Mdc*$^{+/-}$ mice and analyzing 104 pups, we detected no live-born double knockouts, and proportion of *Xlf*$^{-/-}$*Mdc1*$^{+/+}$ and *Xlf*$^{-/-}$*Mdc1*$^{+/-}$ littermates was 36 to 68, which is close to Mendelian distribution 1:2:0. Overall, XLF-deficient mouse and cell line models can be used to identify a set of factors involved in the DNA repair, including the aspects of B and T lymphocyte development and neurodevelopment.

Highlights

Inactivation of *Trp53* gene rescues synthetic lethality between *Xlf* and *Paxx* in mice

Combined inactivation of *Xlf* and *Paxx* leads to severe B and T lymphocytopenia in adult mice

Inactivation of one allele of *Trp53* rescues synthetic lethality between *Xlf* and *Dna-pkcs* genes in mice

Combined inactivation of *Paxx* and *Dna-pkcs* results in live-born fertile *Paxx*$^{-/-}$*Dna-pkcs*$^{-/-}$ mice

Author contribution

SC, MTX, RGF, SS, and VO planned and performed experiments, and interpreted results. VO wrote the paper.

Acknowledgments

This work was supported by the Research Council of Norway Young Talent Investigator grant (# 249774) to VO. In addition, VO group is supported by The Liaison Committee for education, research and innovation in Central Norway (# 13477), the Cancer Society of Norway (# 182355), FRIMEDBIO grants (# 270491 and # 291217), and The Outstanding Academic Fellow Program at NTNU (2017-2021).

Figure legends

Figure 1. Inactivation of *Trp53* rescues synthetic lethality between *Xlf* and *Paxx* in mice. **(A)** Combined inactivation of *Xlf* and *Paxx* leads to synthetic lethality in mice. Both parents were *Xlf*$^{-/-}$*Paxx*$^{+/-}$. **(B)** Live *Xlf*$^{-/-}$*Paxx*$^{-/-}$ embryos were detected at day E15.5. Both parents were *Xlf*$^{-/-}$*Paxx*$^{+/-}$. **(C)** The number of thirty-day-old mice (P30) of indicated genotypes. Both parents were *Xlf*$^{-/-}$*Paxx*$^{+/-}$*Trp53*$^{+/-}$. **(D)** Example of thirty-day-old *Xlf*$^{-/-}$*Paxx*$^{-/-}$*Trp53*$^{-/-}$ and *Xlf*$^{-/-}$*Trp53*$^{-/-}$ female littermates. **(E)** The average weight of thirty-day-old mice in grams. **(F)** Spleens (**left**) and thymi (**right**) isolated from *Xlf*$^{-/-}$*Trp53*$^{-/-}$, *Xlf*$^{-/-}$*Trp53*$^{+/-}$, *Xlf*$^{-/-}$*Paxx*$^{-/-}$*Trp53*$^{+/-}$ and *Xlf*$^{-/-}$*Paxx*$^{-/-}$*Trp53*$^{-/-}$ mice. The weight of spleens **(G)** and thymi **(H)** isolated from thirty-day-old mice of indicated genotypes. Count of splenocytes **(I)** and thymocytes **(J)** isolated from thirty-day-old mice of indicated genotypes. The data from *Xlf*$^{-/-}$*Paxx*$^{-/-}$*Trp53*$^{+/-}$ and *Xlf*$^{-/-}$*Paxx*$^{-/-}$*Trp53*$^{-/-}$ mice are combined in E, G, H, I, J.

Figure 2. Inactivation of *Trp53* rescues synthetic lethality between *Xlf* and *Dna-pkcs* in mice. The number of thirty-day-old (P30) **(A)** and one-day-old (P1) **(B)** mice of indicated genotypes. Both parents were *Xlf*$^{-/-}$*Dna-pkcs*$^{+/-}$*Trp53*$^{+/-}$. **(C)** Body weights of thirty-day-old mice of indicated genotypes. There was no significant difference between WT, *Xlf*$^{-/-}$, *Dna-pkcs*$^{-/-}$, *Trp53*$^{-/-}$, *Xlf*$^{-/-}$*Trp53*$^{-/-}$ and *Dna-pkcs*$^{-/-}$*Trp53*$^{-/-}$ age-matched mice (n.s., p>0.1808). *Xlf*$^{-/-}$*Dna-pkcs*$^{-/-}$*Trp53*$^{+/-}$ mice were similar to *Ku80*$^{-/-}$ mice (n.s., p=0.9442) and smaller than WT, single and double knockout controls (****, p<0.0001).

Figure 3. Combined inactivation of *Paxx* and *Dna-pkcs* results in live-born mice indistinguishable from *Dna-pkcs* knockout controls. **(A)** The number of thirty-day-old mice of indicated genotypes. Both parents were *Paxx*$^{-/-}$*DNA-PKcs*$^{+/-}$ (top) or *Paxx*$^{-/-}$*Dna-pkcs*$^{+/scid}$ (bottom). **(B)** Body weights of thirty-day-old mice of indicated genotypes. There was no significant difference between body weights of WT, *Paxx*$^{-/-}$, *Dna-pkcs*$^{-/-}$ and *Paxx*$^{-/-}$*Dna-pkcs*$^{-/-}$ mice (p>0.6965). **(C)** Sensitization of WT, *PAXX*$^{-}$, *DNA-PKcs*$^{-}$, *PAXX*$^{-}$*DNA-PKcs*$^{-}$, and *XRCC4*$^{-}$ HAP1 cells to doxorubicin at indicated concentrations. Results are from the mean (SD) of three independent experiments. Cell survival (%) represents the relative proportion of the fluorescence normalized to untreated cells. Comparisons between every two groups were made using one-way ANOVA, GraphPad Prizm 7.04. ***PAXX*$^{-}$ *DNA-PKcs*$^{-}$** vs ***DNA-PKcs*$^{-}$**, *p*=0.9992 (n.s.) at 1 nM, and p>0.9999 (n.s.) from 2 nM to 16 nM of doxorubicin. **(D)** Sensitization of WT, *PAXX*$^{-}$, *DNA-PKcs*$^{-}$, *PAXX*$^{-}$*DNA-PKcs*$^{-}$, and *XRCC4*$^{-}$ HAP1 cells to bleomycin at indicated concentrations. Results are from the mean (SD) of three independent experiments. Cell survival (%) represents the relative proportion of the fluorescence to untreated cells. Comparisons between every two groups were obtained using one-way ANOVA, GraphPad Prizm 7.04. ***PAXX*$^{-}$ *DNA-PKcs*$^{-}$** vs ***DNA-PKcs*$^{-}$**, *p*=0.9985 (n.s.) at 0.05 µM, *p*=0.9500 (n.s.) at 0.1 µM, *p*=0.9617 (n.s.) at 0.2 µM, *p*=0.9414 (n.s.) at 0.4 µM, *p*=0.9353 (n.s.) at 0.8 µM, *p*=0.9483 (n.s.) at 1.2 µM, *p*=0.8174 (n.s.) at 1.6 µM of bleomycin.

References

1. Kumar, V., F.W. Alt, and V. Oksenych, *Functional overlaps between XLF and the ATM-dependent DNA double strand break response.* DNA Repair (Amst), 2014. **16**: p. 11-22.
2. Craxton, A., et al., *XLS (c9orf142) is a new component of mammalian DNA double-stranded break repair.* Cell Death Differ, 2015. **22**(6): p. 890-7.
3. Hung, P.J., et al., *MRI Is a DNA Damage Response Adaptor during Classical Non-homologous End Joining.* Mol Cell, 2018. **71**(2): p. 332-342 e8.
4. Ochi, T., et al., *DNA repair. PAXX, a paralog of XRCC4 and XLF, interacts with Ku to promote DNA double-strand break repair.* Science, 2015. **347**(6218): p. 185-188.
5. Xing, M., et al., *Interactome analysis identifies a new paralogue of XRCC4 in non-homologous end joining DNA repair pathway.* Nat Commun, 2015. **6**: p. 6233.
6. Gu, Y., et al., *Growth retardation and leaky SCID phenotype of Ku70-deficient mice.* Immunity, 1997. **7**(5): p. 653-65.
7. Nussenzweig, A., et al., *Requirement for Ku80 in growth and immunoglobulin V(D)J recombination.* Nature, 1996. **382**(6591): p. 551-5.
8. Gago-Fuentes, R., et al., *Normal development of mice lacking PAXX, the paralogue of XRCC4 and XLF.* FEBS Open Bio, 2018. **8**(3): p. 426-434.
9. Oksenych, V., et al., *Functional redundancy between repair factor XLF and damage response mediator 53BP1 in V(D)J recombination and DNA repair.* Proc Natl Acad Sci U S A, 2012. **109**(7): p. 2455-60.
10. Oksenych, V., et al., *Functional redundancy between the XLF and DNA-PKcs DNA repair factors in V(D)J recombination and nonhomologous DNA end joining.* Proc Natl Acad Sci U S A, 2013. **110**(6): p. 2234-9.
11. Xing, M., et al., *Synthetic lethality between murine DNA repair factors XLF and DNA-PKcs is rescued by inactivation of Ku70.* DNA Repair (Amst), 2017. **57**: p. 133-138.
12. Gao, Y., et al., *A critical role for DNA end-joining proteins in both lymphogenesis and neurogenesis.* Cell, 1998. **95**(7): p. 891-902.
13. Frank, K.M., et al., *Late embryonic lethality and impaired V(D)J recombination in mice lacking DNA ligase IV.* Nature, 1998. **396**(6707): p. 173-7.
14. Gao, Y., et al., *A targeted DNA-PKcs-null mutation reveals DNA-PK-independent functions for KU in V(D)J recombination.* Immunity, 1998. **9**(3): p. 367-76.
15. Li, G., et al., *Lymphocyte-specific compensation for XLF/cernunnos end-joining functions in V(D)J recombination.* Mol Cell, 2008. **31**(5): p. 631-40.
16. Kumar, V., F.W. Alt, and V. Oksenych, *Reprint of "Functional overlaps between XLF and the ATM-dependent DNA double strand break response".* DNA Repair (Amst), 2014. **17**: p. 52-63.
17. Abramowski, V., et al., *PAXX and Xlf interplay revealed by impaired CNS development and immunodeficiency of double KO mice.* Cell Death Differ, 2018. **25**(2): p. 444-452.
18. Balmus, G., et al., *Synthetic lethality between PAXX and XLF in mammalian development.* Genes Dev, 2016. **30**(19): p. 2152-2157.
19. Liu, X., et al., *PAXX promotes KU accumulation at DNA breaks and is essential for end-joining in XLF-deficient mice.* Nat Commun, 2017. **8**: p. 13816.
20. Dewan, A., et al., *Robust DNA repair in PAXX-deficient mammalian cells.* FEBS Open Bio, 2018. **8**(3): p. 442-448.
21. Jacks, T., et al., *Tumor spectrum analysis in p53-mutant mice.* Curr Biol, 1994. **4**(1): p. 1-7.
22. Bosma, G.C., R.P. Custer, and M.J. Bosma, *A severe combined immunodeficiency mutation in the mouse.* Nature, 1983. **301**(5900): p. 527-30.
23. Lou, Z., et al., *MDC1 maintains genomic stability by participating in the amplification of ATM-dependent DNA damage signals.* Mol Cell, 2006. **21**(2): p. 187-200.
24. Tadi, S.K., et al., *PAXX Is an Accessory c-NHEJ Factor that Associates with Ku70 and Has Overlapping Functions with XLF.* Cell Rep, 2016. **17**(2): p. 541-555.

25. Gao, Y., et al., *Interplay of p53 and DNA-repair protein XRCC4 in tumorigenesis, genomic stability and development.* Nature, 2000. **404**(6780): p. 897-900.
26. Frank, K.M., et al., *DNA ligase IV deficiency in mice leads to defective neurogenesis and embryonic lethality via the p53 pathway.* Mol Cell, 2000. **5**(6): p. 993-1002.
27. Jiang, W., et al., *Differential phosphorylation of DNA-PKcs regulates the interplay between end-processing and end-ligation during nonhomologous end-joining.* Mol Cell, 2015. **58**(1): p. 172-85.
28. Murga, M., et al., *A mouse model of ATR-Seckel shows embryonic replicative stress and accelerated aging.* Nat Genet, 2009. **41**(8): p. 891-8.
29. Albers, E., et al., *Loss of PICH Results in Chromosomal Instability, p53 Activation, and Embryonic Lethality.* Cell Rep, 2018. **24**(12): p. 3274-3284.
30. Kumar, V., F.W. Alt, and R.L. Frock, *PAXX and XLF DNA repair factors are functionally redundant in joining DNA breaks in a G1-arrested progenitor B-cell line.* Proc Natl Acad Sci U S A, 2016. **113**(38): p. 10619-24.
31. Lescale, C., et al., *Specific Roles of XRCC4 Paralogs PAXX and XLF during V(D)J Recombination.* Cell Rep, 2016. **16**(11): p. 2967-2979.
32. Hung, P.J., et al., *Deficiency of XLF and PAXX prevents DNA double-strand break repair by non-homologous end joining in lymphocytes.* Cell Cycle, 2017. **16**(3): p. 286-295.
33. Liu, X., et al., *Overlapping functions between XLF repair protein and 53BP1 DNA damage response factor in end joining and lymphocyte development.* Proc Natl Acad Sci U S A, 2012. **109**(10): p. 3903-8.
34. Zha, S., et al., *ATM damage response and XLF repair factor are functionally redundant in joining DNA breaks.* Nature, 2011. **469**(7329): p. 250-4.

Post-print version of paper by Castaneda-Zegarra et al., published in DNA repair journal (Amst.) 2019 Jan;73:164-169. doi: 10.1016/j.dnarep.2018.12.002. Epub 2018 Dec 16. PMID: 30579708

Figure 1

A

Genotype	Number of offsprings, P30	Expected, 1:2:0
Xlf$^{-/-}$*Paxx*$^{+/+}$	14	15
Xlf$^{-/-}$*Paxx*$^{+/-}$	31	30
Xlf$^{-/-}$*Paxx*$^{-/-}$	0	0
Total	45	45

B

Genotype	Number of embryos, E15.5	Expected, 1:2:1
Xlf$^{-/-}$*Paxx*$^{+/+}$	8	8
Xlf$^{-/-}$*Paxx*$^{+/-}$	18	16
Xlf$^{-/-}$*Paxx*$^{-/-}$	6	8
Total	32	32

C

Genotype	Number of offsprings, P30	Expected, 1:2:1:2:4:2:1:2:1
Xlf$^{-/-}$*Paxx*$^{+/+}$*Trp53*$^{+/+}$	7	5.2
Xlf$^{-/-}$*Paxx*$^{+/+}$*Trp53*$^{+/-}$	14	10.4
Xlf$^{-/-}$*Paxx*$^{+/+}$*Trp53*$^{-/-}$	7	5.2
Xlf$^{-/-}$*Paxx*$^{+/-}$*Trp53*$^{+/+}$	11	10.4
Xlf$^{-/-}$*Paxx*$^{+/-}$*Trp53*$^{+/-}$	27	20.8
Xlf$^{-/-}$*Paxx*$^{+/-}$*Trp53*$^{-/-}$	6	10.4
Xlf$^{-/-}$*Paxx*$^{-/-}$*Trp53*$^{+/+}$	**0**	**5.2**
Xlf$^{-/-}$*Paxx*$^{-/-}$*Trp53*$^{+/-}$	**7**	**10.4**
Xlf$^{-/-}$*Paxx*$^{-/-}$*Trp53*$^{-/-}$	**4**	**5.2**
Total	83	83

D

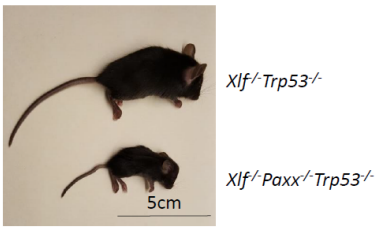

F

E

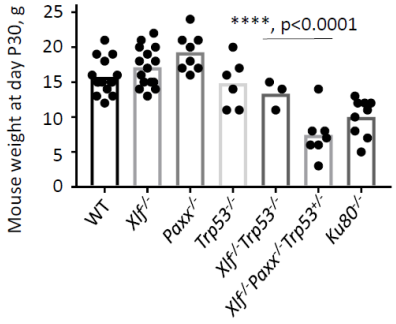

G

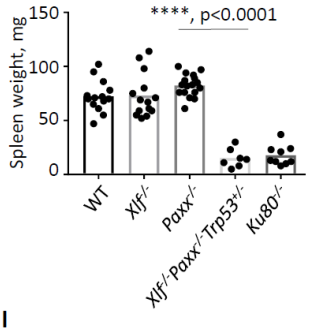

H

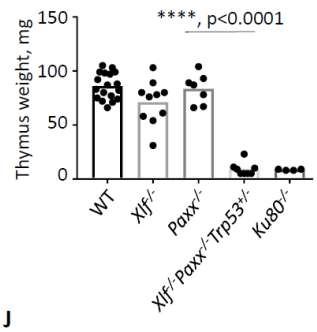

I

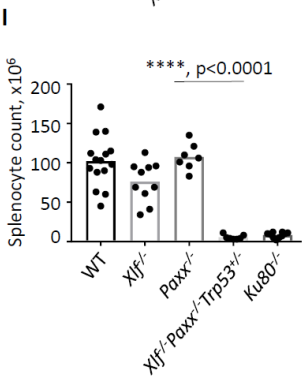

J

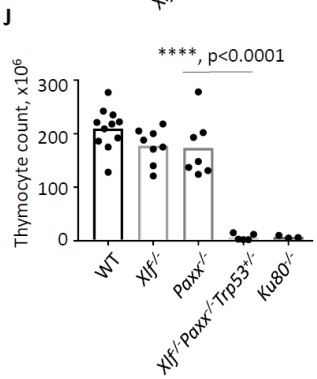

Post-print version of paper by Castaneda-Zegarra et al., published in DNA repair journal (Amst.) 2019 Jan;73:164-169. doi: 10.1016/j.dnarep.2018.12.002. Epub 2018 Dec 16. PMID: 30579708

Figure 2

A

Genotype	Number of offsprings, **P30**	Expected at P30, 1:2:1:2:4:2:1:2:1
Xlf$^{-/-}$*Dna-pkcs*$^{+/+}$*Trp53*$^{+/+}$	35	20.5
Xlf$^{-/-}$*Dna-pkcs*$^{+/+}$*Trp53*$^{+/-}$	43	41.0
Xlf$^{-/-}$*Dna-pkcs*$^{+/+}$*Trp53*$^{-/-}$	24	20.5
Xlf$^{-/-}$*Dna-pkcs*$^{+/-}$*Trp53*$^{+/+}$	54	41.0
Xlf$^{-/-}$*Dna-pkcs*$^{+/-}$*Trp53*$^{+/-}$	97	82.0
Xlf$^{-/-}$*Dna-pkcs*$^{+/-}$*Trp53*$^{-/-}$	49	41.0
Xlf$^{-/-}$*Dna-pkcs*$^{-/-}$*Trp53*$^{+/+}$	0	20.5
Xlf$^{-/-}$*Dna-pkcs*$^{-/-}$*Trp53*$^{+/-}$	25	41.0
Xlf$^{-/-}$*Dna-pkcs*$^{-/-}$*Trp53*$^{-/-}$	1	20.5
Total	**328**	328

B

Genotype	Number of offsprings, **P1**	Expected at P1, 1:2:1:2:4:2:1:2:1
Xlf$^{-/-}$*Dna-pkcs*$^{+/+}$*Trp53*$^{+/+}$	9	7
Xlf$^{-/-}$*Dna-pkcs*$^{+/+}$*Trp53*$^{+/-}$	15	14
Xlf$^{-/-}$*Dna-pkcs*$^{+/+}$*Trp53*$^{-/-}$	7	7
Xlf$^{-/-}$*Dna-pkcs*$^{+/-}$*Trp53*$^{+/+}$	12	14
Xlf$^{-/-}$*Dna-pkcs*$^{+/-}$*Trp53*$^{+/-}$	36	28
Xlf$^{-/-}$*Dna-pkcs*$^{+/-}$*Trp53*$^{-/-}$	17	14
Xlf$^{-/-}$*Dna-pkcs*$^{-/-}$*Trp53*$^{+/+}$	4	7
Xlf$^{-/-}$*Dna-pkcs*$^{-/-}$*Trp53*$^{+/-}$	12	14
Xlf$^{-/-}$*Dna-pkcs*$^{-/-}$*Trp53*$^{-/-}$	0	7
Total	**112**	112

C

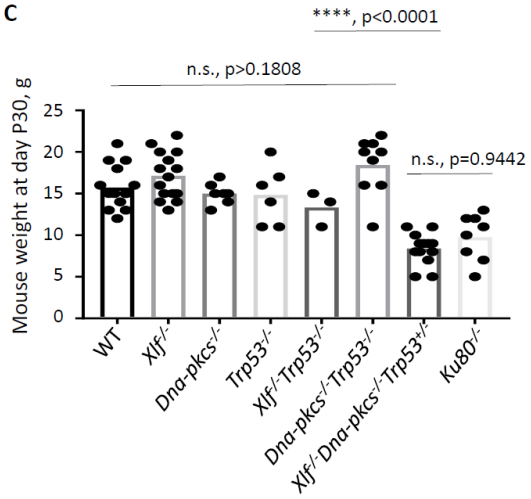

Post-print version of paper by Castaneda-Zegarra et al., published in DNA repair journal (Amst.) 2019 Jan;73:164-169. doi: 10.1016/j.dnarep.2018.12.002. Epub 2018 Dec 16. PMID: 30579708

Figure 3

A

Genotype	Number of offspring, P30	Expected, 1:2:1
Paxx$^{-/-}$*Dna-pkcs*$^{+/+}$	28	29
Paxx$^{-/-}$*Dna-pkcs*$^{+/-}$	63	59
Paxx$^{-/-}$*Dna-pkcs*$^{-/-}$	26	29
Total	117	117
Paxx$^{-/-}$*Dna-pkcs*$^{+/+}$	19	18
Paxx$^{-/-}$*Dna-pkcs*$^{+/scid}$	40	36
Paxx$^{-/-}$*Dna-pkcs*$^{scid/scid}$	13	18
Total	72	72

B

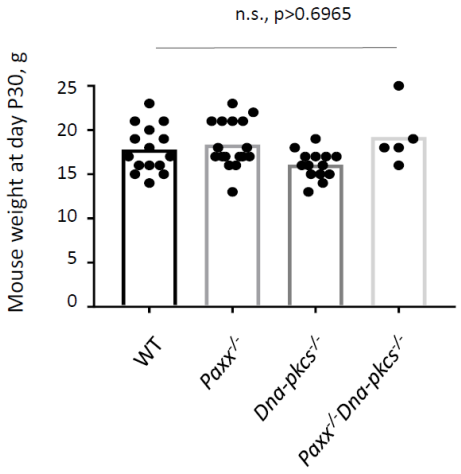

C

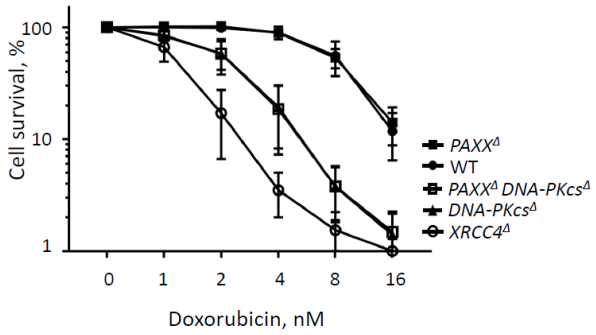

D